HEAT TRANSFER IN THE ATMOSPHERE

J. Oerlemans

Institute for Meteorology and Oceanography, University of Utrecht
Princetonplein 5, Utrecht, The Netherlands

ABSTRACT

The atmosphere is almost transparent to solar radiation and almost opaque to terrestrial radiation. This implies that in the mean the atmosphere cools while the earth's surface is heated. Convection in the lower atmosphere must therefore occur. The upward flux of energy associated with it is large in the equatorial regions and very small at high latitudes. Balance requirements then demand an energy flux from the equator to the poles, which is accomplished by large-scale atmospheric motions and ocean currents.

This review concentrates on the nature of radiative transfer in the atmosphere, atmospheric motions that redistribute energy over the globe, and energy transfer in the convective boundary layer.

1. INTRODUCTION

In most atmospheric phenomena heat transfer plays an important, if not governing, role. The large-scale structure of the lower atmosphere is dominated by the equator-to-pole temperature gradient. In some way, this gradient measures the potential energy that is in principle available for conversion to kinetic energy. We know from observations that atmospheric disturbances continuously grow at the expense of the potential energy reservoir mentioned above. A well-known example of such a disturbance is the midlatitude storm (depression), which generates a considerable amount of kinetic energy (although it is only a fraction of the available potential energy). The kinetic energy is then dissipated by both internal and surface friction.

To feed the potential energy reservoir, and ultimately the dissipation, differential heating is a necessity. It is accomplished by the large difference in solar heating between low and high latitudes. There is another, and in fact more proper way to put it: due to the constitutive laws which the atmosphere obeys, differences in heating must create motions. These motions have the capability to transport energy, making it possible to achieve an energy balance that deviates from local radiative equilibrium.

So solar energy drives the general circulation of the atmosphere. To understand the way in which the atmosphere is heated, it is necessary to examine the radiative properties of the atmosphere. This is not so easy, because the atmosphere is a mixture of gases, and many of them are radiatively active.

At this point it is convenient to introduce the concept of tropopause, which separates the lower part of the atmosphere (the troposphere) from the upper part. This tropopause appears as a sharp increase in the stability of the stratification (going upward); its height varies from about 8 km at the poles to about 16 km in the equatorial regions. In the troposphere the air is relatively well mixed, as long as water vapour is not considered. We will examine how a dry atmosphere can be in radiative equilibrium. If water vapour is added things become much more complex. With regard to the radiation emitted by bodies at a temperature typical for our climate ($200 < T < 300$ K, say), water vapour is very active. In computing radiative heat fluxes this would not be a problem if the distribution of water vapour would be uniform, or at least constant in time. However, the opposite is the case: the concentration of water vapour varies highly in space and time.

Above the tropopause, the most important feature is the ozone layer, which extends from about 15 to about 40 km. Here a substantial amount of solar radiation is absorbed, which explains the high temperatures found at these heights ($T \simeq 240$ K, about 20 K higher than T at the tropopause). The chemistry of the upper atmosphere is complex and not yet understood. In this review we will not discuss it.

In a first approximation, the atmosphere is opaque to terrestrial radiation and almost transparent to solar radiation. As a consequence, the (global and annual mean) troposphere cools while the surface is heated up. This obviously leads to an unstable stratification in the boundary layer and thus to the development of convection. Heating of the troposphere is mainly due to convection, involving an upward flux of both sensible and latent heat (water vapour). The ratio of the sensible heat to the latent heat flux is known as the Bowen ratio B. In the tropics it is smaller than 0.1, so the latent heat flux accounts for the bulk of the upward energy flux. It is only at very high latitudes or in very dry regions that $B > 1$.

Convection in the atmosphere is complex for

two reasons. First, steady states hardly occur. One always has to deal with growing or decaying convective boundary layers. Second, the presence of water, or better, its phase transitions, have a very profound effect on the energetics of the convection.

The overview given above is incomplete and disorderly. Nevertheless, when it has given the impression that atmospheric heat transfer has many aspects, it has served the purpose. So how to proceed ? Instead of skipping through a long list of atmospheric processes involving heat transfer, we concentrate on three topics:

(i) The nature of radiative transfer in the troposphere and the implications for climate dynamics.

(ii) How the differences in heating over the globe force atmospheric motions, and how these motions restore the energy balance.

(iii) Heating of the atmosphere by convection.

In this way we catch the most important ingredients of the climate system, namely, the heat fluxes from equator to pole and from surface to atmosphere, balancing the radiative heating or cooling.

2. RADIATIVE TRANSFER IN THE ATMOSPHERE

Since the radiation temperature of the sun and the earth are very different (about 5700 K and 250 K, respectively), the spectra of their black body radiation hardly show any overlap. Solar radiation is mainly in the 0.2 - 3 μm range, while terrestrial radiation has wavelengths between 3 and 100 μm. In simple radiation models for the atmosphere it is common practice to treat solar and terrestrial radiation as independent and separated matters. We will now discuss extremely simple models. The theory of radiative transfer in the atmosphere is well developed, but only a fraction of this is needed to understand the basic effects of radiation on the climate system. For a general treatment of radiative processes in meteorology, see Paltridge and Platt (1976).

In a long-term global balance, the amount of solar radiation absorbed by the earth and its atmosphere should equal the net outgoing terrestrial radiation. This defines an effective radiation temperature of the earth-atmosphere system:

$$(1) \qquad T = \left[S(1-\alpha)/4\sigma\right]^{1/4} .$$

S is the solar constant (1365 W/m^2), α the mean planetary albedo (0.3) and σ the Stefan-Boltzmann constant. The factor 1/4 accounts for the fact that the solar radiation is distributed over an area which is 4 times the area that intercepts the solar beam. From eq. (1) we find T=255 K. This is considerably lower than the observed mean surface temperature (about 287 K), and we have to conclude that the atmosphere plays an important role. Apparently, the terrestrial radiation as seen from space finds its origin somewhere in the atmosphere. The atmosphere absorbs the longwave radiation from the surface and emits it again both up- and downwards, at a lower temperature (the greenhouse effect). Let us examine this in somewhat more detail by constructing a two-layer model of the earth-atmosphere system.

We treat the atmosphere as a whole, and assume that it absorbs a fraction A_a of the incoming solar flux. Its radiative properties for terrestrial radiation are completely determined by a constat bulk emissivity ϵ (grey body approximation). The earth surface absorbs a fraction A_s of the incoming solar energy and radiates as a black body. A dynamic heat flux couples the surface and atmosphere. We assume that it has the form $K(T_s-T_a)$, where K is an exchange coefficient, T_s surface temperature and T_a a (characteristic) atmospheric temperature.

In a steady state, the heat fluxes at the top of the atmosphere and at the surface must be zero. This yields

$$(2) \qquad S'(A_a+A_s) - (1-\epsilon)\sigma T_s^4 - \epsilon\sigma T_a^4 = 0 ,$$

$$(3) \qquad S'A_s + \epsilon\sigma T_a^4 - \sigma T_s^4 - K(T_s-T_a) = 0 .$$

S/4 is replaced by S'. Even if K would be a constant, which is definitely not the case, this system is diificult to solve without numerical methods. It is instructive, however, to consider the case with K=0. We then have

$$(4) \qquad T_s^4 = S'(2A_s+A_a)/(2-\epsilon) ,$$

$$(5) \qquad T_a^4 = S'(A_s+A_a/\epsilon)/(2-\epsilon) .$$

From eq. (4) we see that surface temperature increases if the emissivity of the atmosphere increases. Also, the surface is warmer than the atmosphere if $A_s/A_a > (1-\epsilon)/\epsilon$.

Typical values for the absorption of solar radiation are A_s=0.5 and A_a=0.2, consistent with the planetary albedo of about 0.3. The estimated value of ϵ is 0.91. Inserting these values in eqs. (4) and (5) yields T_s=285 K and T_a=251 K, which is remarkably close to the observed temperatures. So it seems that the upward dynamical heat flux is insignificant. However, this conclusion is wrong because better models show that the error made by neglecting the upward heat flux cancels the error caused by the poor resolution of the model (one layer for the whole atmosphere).

Pioneering work on multilevel models of radiation in the atmosphere was done by Manabe and Wetherald (1967). Their approach has been extended by many workers. An interesting recent paper on this matter is Ramanathan (1981).
We will not discuss such models here.

One mechanism that makes the climate system interesting is the temperature albedo feedback. Lower surface temperatures lead to a more extensive snow and ice cover and this to an increased albedo α . The consequences of this feedback can be studied with the simplest climate model possible, namely, eq. (1). So let us include albedo feedback in eq. (1), and see what type of nonlinear structure shows up.

3. GLOBAL STRUCTURE OF A CLIMATE SYSTEM WITH ALBEDO FEEDBACK

In a zero-dimensional (global mean) climate model, dynamical energy transports do not appear in the energy balance. Including albedo feedback makes it necessary to use surface temperature T_s as state variable. To solve a radiation balance for T_s , both absorption of solar radiation and net emission of terrestrial radiation must be expressed in terms of T_s. This only makes sense if the vertical temperature structure of the atmosphere is invariant under climatic change. Otherwise, T_s will not properly represent the climatic state. Evidence exists that such a requirement is reasonably well met (e.g. there is not much reason to believe that the stratification in the atmosphere will change substantially if the solar constant S drops by a few per cent).

The solid line in Figure 1 shows how the absorption of solar radiation depends on T_s. The arctangens-shaped curve reflects the effect of the temperature-albedo feedback. For low T_s, the earth is completely covered with ice and snow ($\alpha \simeq 0.7$). For high T_s, there is no snow or ice cover at all. We measure the strength of the albedo feedback by s, the maximum slope of the absorption curve.

The dashed line represents the (linearized) net loss of energy by terrestrial radiation, given by $a+bT_s$. A first estimate of a and b can be obtained by linearizing the longwave contribution in eq. (2) around some characteristic temperature. It appears that this yields a value for b which is larger than the one suggested by data from satellite measurements. The reason for this is the dependence of atmospheric water vapour content on temperature. An increasing temperature will of course increase the emission of longwave radiation, but at the same time the higher concentration of water vapour leads to a larger value of ϵ (atmospheric emissivity). So the counter radiation also increases, and the net effect of the temperature increase on the emission of longwave

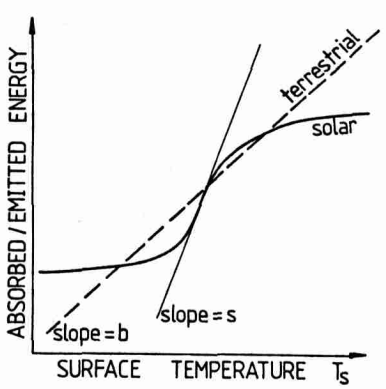

Figure 1. Components of the radiation balance for a climate model with state variable T_s.

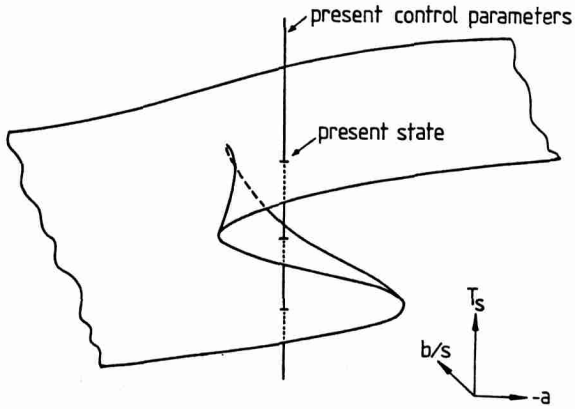

Figure 2. Equilibrium manifold for the zero-dimensional climate model.

energy is reduced. The presence of water vapour thus reduces the value of b. In other words, it enhances climate sensitivity: a larger change in T_s is required to restore a perturbed radiation balance. At this point we do not yet specify a and b, but examine how the climate model behaves if these parameters vary.

Equilibria are found by equating the absorbed solar energy to the energy loss by terrestrial radiation, i.e. by looking at the intersections of the solid and dashed curves in Figure 1. The number of intersections is one or three, depending on the specific values of a, b and s.

First of all, three equilibria are possible only if $b < s$. Otherwise one equilibrium exists, which is stable. We also observe that for each value of b, critical values a_+ and a_- exist such that one and only one equilibrium is possible if $a \geq a_+$ or $a \leq a_-$. So the relevant control parameters are b/s and a. At a set of points in the (a,b/s)-control plane bifurcation (one equilibrium $\leftrightarrow$ three equilibria) occurs. It thus appears that the structure of this climate model is completely described by Thom's second elementary catastrophe (the cusp catastrophe, Thom, 1975; for an enligthening discussion on catastrophe theory, see Gilmore, 1981). The equilibrium climatic states form a two-dimensional manifold in $(T_s, a, b/s)$-space, see Figure 2.

To determine the position of the present climatic state on the manifold, estimates of a, b and s should be available. Such estimates can be obtained from more sophisticated climate models, which are tuned with the aid of satellite measurements on albedo, longwave radiation and cloud cover (e.g. Oerlemans and Van den Dool, 1978). It appears that we are on the warm side in the three-equilibria region, as indicated in Figure 2. The cold equilibrium possible with the present control parameters corresponds to a completely ice-covered earth. No evidence exists that the earth has ever been in such a state.

The picture of the global radiation regime sketched above forms a framework. Effects of increasing CO_2 concentration, changing solar constant,

variations in cloudiness, etc., can be studied by adjusting the control parameters a, b and s. In most cases it requires detailed modelling to find how the control parameters change. The role of clouds, in particular, is a matter of continuous debate.

So far we considered the global climate system. If some part of it is investigated (north of 50° lat., say) energy transport has to be taken into account. When the amount of heat gained from convergence of the dynamic heat flux can be set proportional to the temperature in that region (e.g. the polar regions receive more heat from the tropics if temperature is lower), the qualitative behaviour of T_s is still governed by a cusp catastrophe. The effect of the heat flux convergence is to steepen the dashed line in Figure 1, so the three-equilibria region shrinks. Experiments with latitude-dependent climate models suggest that the effect of the poleward heat flux is so large that higher latitudes cannot be locked in the cold equilibrium.

4. LARGE-SCALE MOTIONS IN THE ATMOSPHERE

Since the amount of solar energy received at lower latitudes is considerably larger than that received at higher latitudes, a state of radiative equilibrium would imply a very large equator-to-pole temperature gradient. However, the associated differences in air density create a north-south pressure gradient forcing motion and therewith heat transfer. So pure radiative equilibrium is not possible.

Disregarding the fact that the earth is rotating, the simplest energy balance is the one associated with a circulation as shown in Figure 3. Since in the tropopshere potential temperature (temperature corrected for adiabatic expansion due to vertical motion) increases with height, upward motion cools the air while downward motion warms it. So in the circulation of Figure 3, upward motion in the warm tropical troposphere counteracts the net diabatic heating. At high latitudes, downward motion counteracts the net diabatic cooling. The remaining difference in heating rate is taken

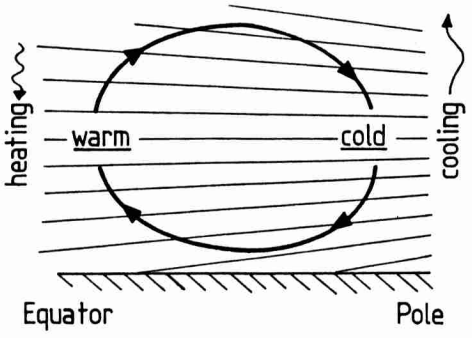

Figure 3. Tropospheric circulation conserving energy in case of hydrostatic balance. Thin lines are isobars.

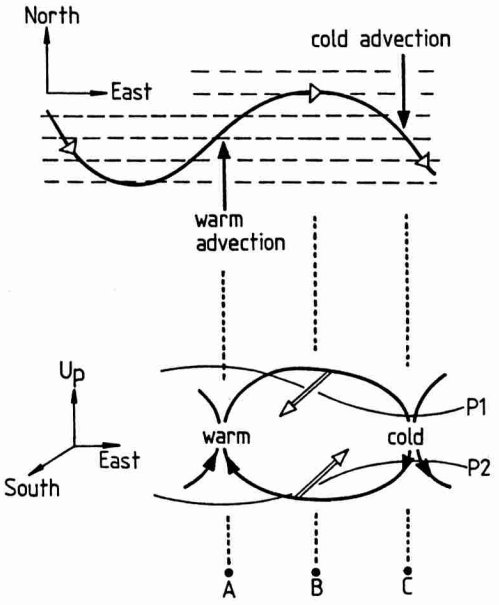

Figure 4. Dynamics of a perturbation on the zonal (i.e. east-west) flow. See text for explanation.

care of by the heat flux associated with the horizontal flow. In order to maintain the circulation against friction, the net effect of the pressure force must be acceleration of the flow. This is achieved if the polar troposphere is colder than the equatorial troposphere (in case of hydrostatic balance). The associated vertical spacing of pressure levels (thin lines in the figure) decreases towards the pole, of course.

The earth's rotation modifies this circulation considerably. The Coriolis force acts perpendicular to the velocity of a particle (with the back upstream, the force is to the right in the Northern Hemisphere). So the upper-level flow in Figure 3 will have a strong westerly component (it blows towards the east), whereas the lower-level flow will have an easterly component. This type of circulation is named a Hadley cell.

In the absence of friction and curvature of the air-parcel trajectory, and assuming that the pressure force is constant, the Coriolis force will ultimately balance the pressure force exactly. This situation is known as geostrophic balance or geostrohic equilibrium and implies that the wind blows parallel to the isobars. In that case there is no production of kinetic energy. Atmospheric motions with a characteristic scale of 1000 km or more are always close to geostrophic equilibrium (except in the tropics, where the horizontal component of the Coriolis force is small). Such motions are said to be quasi-geostrophic. Small deviations from geostrophic equilibrium account for the generation of kinetic energy. So one can state that the presence of the Coriolis force causes the atmosphere to be an inefficient engine: large differential heating results in a comparatively small amount of kinetic energy. Consequently, dissipation is small compared to radiative heating/cooling.

In reality, a Hadley cell from equator to pole does not exist. The reason is that such a cell is not efficient in transporting heat polewards. A strong south-north temperature gradient remains, so strong that the occurrence of baroclinic instability is rule (perturbations on the zonal flow grow by converting potential energy to kinetic energy).

Figure 4 illustrates this point. In the upper part the dashed lines represent isotherms (and isobars) corresponding to a perfectly geostrophic Hadley cell. So the basic flow is in zonal direction. Let us suppose that for some reason a wavy perturbation is generated in this flow (heavy line with open arrows). This causes a northward flux of warm air at A and a southward flux of cold air at C. The warm air will rise and the cold air will sink, thus establishing a cell circulation as shown in the lower part of Figure 4. In this cell circulation potential energy is converted into kinetic energy. In case of instability, this kinetic energy should enforce the temperature advection. However, the east-west pressure gradient is zero at A and C, and reaches a maximum value at B. So meridional (i.e. south-north) flow is generated at B (remember the Coriolis force), but not at A and C. This means that the perturbation will not grow: the cell circulation has the wrong phase.

At this point it is important to realize that the speed of the basic zonal flow changes with height. This is obvious from Figure 3. As a consequence, the phase of the wavy temperature perturbation is forced to change with height.

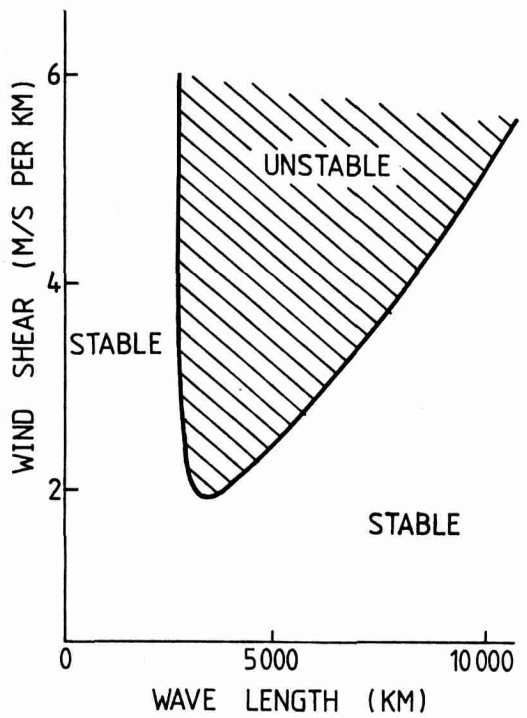

Figure 5. Stability of baroclinic waves.

Since pressure essentially is a (vertical) integral quantity of temperature, pressure and temperature perturbations become out of phase. This effectively produces a shift in the location of the cell circulation, and if the wave is tilted westward with height this shift is in the right direction (the wave will grow). For an extensive discussion on the structure of baroclinic waves in the atmosphere, see Holton (1972).

The first models of baroclinic instability are due to Charney (1947) and Eady (1949). In recent years many refinements have been made (spherical geometry, varying basic state, etc.), both in analytical and numerical modelling. The results of various approaches have much in common and are summarized in Figure 5.

In interpreting Figure 5, it should first be realized that the presence of a south-north temperature gradient implies vertical shearing of the zonal wind. This is a consequence of the fact that pressure is hydrostatic and wind is quasi-geostrophic. So the vertical axis in the figure also represents the meridional temperatrue gradient. It appears that for a given mean zonal wind (labels give values of this quantity) a stable and an unstable region exist. Only in the unstable region conversion from potential to kinetic energy is positive and baroclinic waves grow. For large zonal winds the region of instability becomes narrower. However, the wave length of maximum instability is always in the 3500 to 5000 km range (which is in accordance with observations).

The growth rate χ of the most unstable wave as derived from a simple two-layer model (e.g. Holton, 1972) is

$$(6) \quad \chi^2 = C_1\left(\frac{\partial T}{\partial \phi}\right)^2 - C_2 \sigma^2 \, / \mathrm{tg}\, \phi ,$$

where C_1 and C_2 are constants, ϕ is latitude, $\partial T/\partial \phi$ is the south-north temperature gradient, and σ measures the static stability of the stratification (for stable conditions $\sigma > 0$). As expexted, the growth rate increases with increasing temperature gradient. A larger static stability, on the other hand, reduces the growth rate. Eq. (6) also shows that baroclinic instability will be a more vigorous mechanism at higher latitudes.

The presence of baroclinic instability dominates mid-latitude weather maps. Storms form continuously, and create zones of strong winds and precipitation (in the regions of ascending air). Calculating the formation and evolution of such weather systems is a major aim of numerical weather prediction.

Baroclinic waves possess a remarkable fine structure. Sharp frontal zones and narrow jets frequently occur. The release of latent heat by condensation, associated with regions of potential instability in the warm air, may intensify the storm considerably. In this way the midlatitude storm has a very strong impact on the heat and water vapour budgets of the atmosphere.

5. THE ENERGY CYCLE

Baroclinic waves are very efficient in transporting heat polewards, so efficient that the south-north temperature gradient is rarely larger than its critical value (the smallest value for which instability may occur, see Figure 5). This observation has led to the concept of baroclinic adjustment (Stone, 1978): in middle and high latitudes the zonal mean south-north temperature gradient is always close to its critical value.

A global picture of the actual circulation system in the troposphere is given in Figure 6. At latitudes smaller than about 30° , the Hadley cell dominates. Meridional overturning produces some kinetic energy. Poleward of 30° latitude we find the baroclinic wave regime. Here eddies form continuously, and the flow has characteristics of two-dimensional turbulence. Most of the generated eddy kinetic energy is dissipated, but part of it is given to the zonal flow (the eddies feed the zonal jet !). To maintain hydrostatic and geostrophic conditions, a large temperature gradient must exist in the vicinity of the jet. To establish this gradient, 'reversed overturning' occurs: warm air sinks and cold air rises. So in this circulation, the so-called Ferrel cell, kinetic energy is converted into potential energy. The Ferrel cell cannot be seen on a ordinary weather map, but only appears in the long-term mean flow. Finally, in the polar regions a shallow cell circulation is sometimes present. It is a small Hadley cell, driven by the strong radiative cooling over the polar regions. This cell is weak, however, in particular over the Arctic.

The energy budget of the atmospheric circulation is summarized in Figure 7. The generation of available potential energy amounts to 2 W/m^2 (annual mean value). Apparently, baroclinic waves, including more or less stationary waves forced by ocean-continent contrasts, account for the production of kinetic energy (sometimes referred to as eddy kinetic energy). Most of it is dissipated, but a small part is used to feed the zonal flow. It should be realized that Figure 7 represents a long-term mean picture. Even from year to year changes in the energy reservoirs occur.

It is noteworthy that the amount of kinetic energy in the system is much smaller than the amount of available potential energy. Moreover,

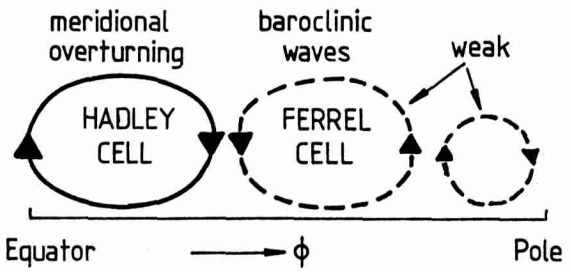

Figure 6. A schematic picture of the circulation regimes in the troposphere.

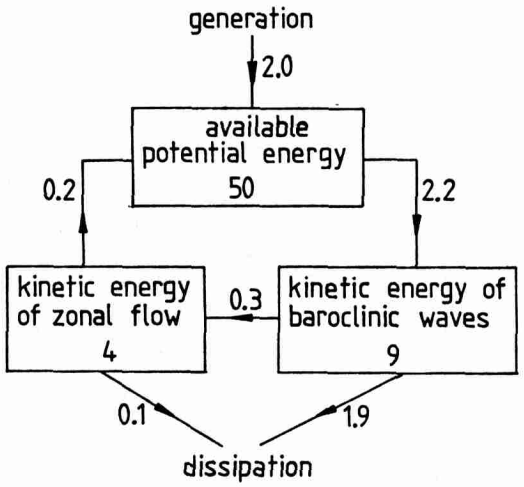

Figure 7. The atmospheric energy cycle. Unit for energy reservoirs is 10^5 J/m^2; for energy conversions (arrows) W/m^2.

dissipative heating is two orders of magnitude smaller than the average heating by solar radiation. This demonstrates the low efficiency of the atmospheric heat engine.

The first comprehensive observational study on the atmospheric energy cycle was carried out by Oort (1964). An impressive text on the nature of the general circulation of the atmosphere was written by Lorenz (1967).

6. CONVECTION IN THE ATMOSPHERE

As discussed earlier in this paper, the global mean radiation balance of the atmosphere is negative while that of the earth's surface is positive. A net upward heat flux is thus required. This heat flux is almost completely established by convection. Over the tropical oceans this happens in a regular way (except for the formation of tropical hurricanes !), but at higher latitudes convection over the ocean is concentrated in outbreaks of cold polar air. In that case cold polar flows equatorwards over warm water and becomes extremely unstable. In particularly over the northern part of the Atlantic Ocean such situations occur frequently.

Over land convection is dominated by the action of the daily cycle in radiation. On each sunny day the convective boundary layer is created in the morning, grows during the day, and disappears again during the night. Consequently, steady state convective boundary layers do not occur over land.

Let us first consider dry convection (the air does not contain water vapour) on a clear day in summer. Due to nocturnal cooling the air just above the surface will be cold at sunrise. The

upper boundary of the cold layer is generally sharp. It appears as a discontinuity in the temperature profile, see Figure 8. Above the cold layer temperature decreases slowly with height. The initial profile shown in Figure 8 represents a stable stratification, i.e. the potential temperature θ increases with height everywhere (lines of constant θ have a slope of 10 K/km in a height-temperature diagram).

Shortly after sunrise, when the radiation balance at the surface becomes positive, heat is added to the cold layer. A well-mixed (θ constant) convective layer is established which grows steadily. The simplest model describing this situation is

$$\dot{h} = \dot{\theta}_m / \gamma_\theta = H^\uparrow / h \gamma_\theta \qquad (7)$$

Here a dot denotes a time derivative, $H^\uparrow$ is the upward heat flux at the surface, h is the thickness of the mixed layer and γ_θ (h) is the actual potential temperature gradient at height h. This model is known as the 'encroachment model' and is frequently used to make a back-of-the-envelope prediction of the maximum surface temperature. However, testing the performance of eq. (7) by comparison to observations shows that calculated values of h(t) are systematically too small (Driedonks, 1981). Apparently, the effect of entrainment at the top of the convective layer is not negligable.

More refined models have been constructed in which the entrainment is parameterized in terms of the kinetic energy budget of the convective layer. Two sources of kinetic energy should be distinguished: convective turbulence generated by buoancy forces (and driven by $H^\uparrow$), and mechanical turbulence due to the effect of friction on the mean horizontal wind. Tennekes (1973) proposed a model of the form

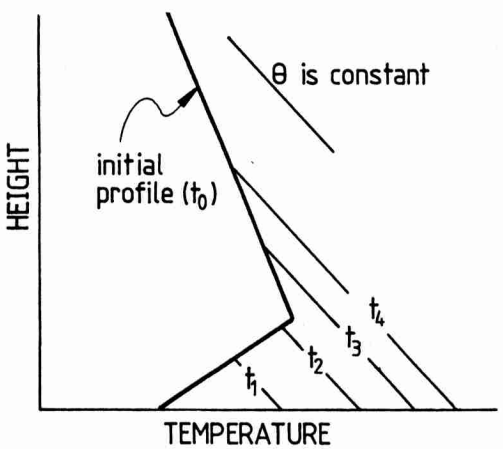

Figure 8. Growth of a well-mixed layer (θ = potential temperature is constant) in a stably stratified atmosphere, which is heated from below. The cold layer at t_o is due to nocturnal cooling.

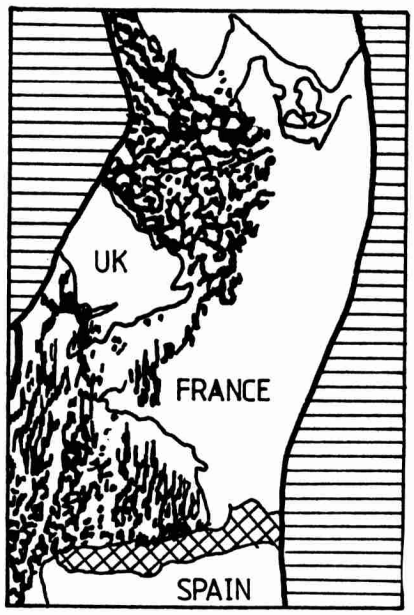

Figure 9. Sketch of a satellite picture made by the NOAA-6 satellite on 13 january 1981. Horizontal shading represents uniform frontal clouds. Convective clouds are shown in black, they are found in the cold outbreak between the frontal zones. The cross-hatched area is a band of very heavy convective activity, caused by forced ascent (upslope precipitation).

$$\dot{h} = (k_1 H^\uparrow + k_2 u_*^3) / h \gamma_\theta \quad , \qquad (8)$$

where k_1 and k_2 are constants, and u_* is the friction velocity. The latter is defined as the square root of the downward momentum flux (which can be estimated if the surface roughness is known. Eq. (8) has been tested against observations and works quite well. Many refinements of this model have been proposed, but the improvements are marginal.

In many regions on this earth sunny day with a dry and stable atmosphere are exceptional. So let us now turn to the more general case in which water vapour is present and the atmosphere is unstable over a depth of a few kilometers.

The presence of water vapour has a strong influence on the dynamics of the convection. This makes a theoretical treatment more difficult, but has also advantages: liquid water in the form of cloud droplets is an excellent visual tool in determining whether motions are up- or downward. We can learn a lot about the structure of convection by just looking at clouds during a walk, or at cloud patterns as seen by satellites. Figure 9 provides an example. It is a sketch of a satellite picture on which several cloud systems can be seen. In this winter situation, convective clouds form because cold air from the north flows over warm water. Note the presence of

both roll and cellular structures. Rolls dominate over the Gulf of Biscay, whereas cellular patterns occur over the North Sea. Except for large-scale frontal clouds, land regions are almost free of clouds.

As stated above, the presence of water vapour has important dynamical consequences. First, water vapour is lighter than dry air, so the buoyancy of an air parcel increases with humidity. Second, latent heat release in moist ascending air represents a substantial source of energy. This is illustrated by the fact that saturated rising air cools 6 K per km, while dry air cools 10 K per km. So if the vertical temperature gradient of the environment is between 6 and 10 K per km, an upward moving air parcel will accelerate if it contains sufficient water vapour (the release of latent heat keeps its buoyancy positive). This situation is known as conditional instability and occurs frequently in the atmosphere.

7. CLOUD STRUCTURE FROM NUMERICAL MODELING

Modern computers have become so fast that detailed numerical simulation of convective clouds is very well possible. It may help a lot in understanding the structure of convective clouds, since detailed observational studies are limited (field experiments involving aircrafts is an expensive matter; recent developments in radar technology seem promising, however).

A class of numerical models widely used is based on the anelastic equations of motion for a continuum. It involves the assumptions that the air is incompressible (density variations only occur as a result of temperature variations), and that horizontal pressure gradients are negligable. In addition to this, only motion in a vertical plane is considered. Let us have a somewhat closer look at this type of model.

Conservation of momentum reads (in Eulerian formulation)

$$(9) \qquad \frac{\partial \vec{v}}{\partial t} + \vec{v}.\nabla\vec{v} = \vec{B} + \nu\nabla^2\vec{v} \ ,$$

and incompressibility requires

$$(10) \qquad \nabla.\vec{v} = 0 \ .$$

Here, $\vec{v}$ is the two-dimensional velocity vector (in a vertical plane), ∇ the two-dimensional gradient operator, $\vec{B}$ the buoyancy force, and ν an eddy diffusion coefficient. The latter should model the effect of eddies that are not resolved by the model. The buoyancy force, which is the only driving force in this model, depends on air temperature, amount of water vapour and amount of liquid water (in the form of cloud droplets). Eqs. (9) and (10) are supplemented by equations for water vapour mixing ratio and liquid water mixing ratio. When supersaturation occurs condensation takes place.

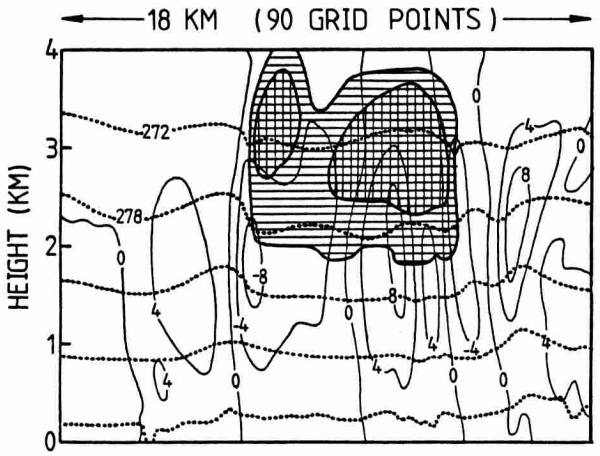

Figure 10. A convective cloud simulated with a numerical model. Hatched regions contain liquid water (cloud droplets). Dotted lines are isotherms (K) and solid lines show vertical motion (m/s, upward is positive).

When cloud droplets are present and the air is not saturated, evaporation occurs. Water vapour and liquid water are also subject to advection by the flow, and to diffusion by the small-scale eddies.

Models of this type contain many nonlinearities and have to be solved numerically. This is usually done by finite difference methods. Figure 10 shows a typical model cloud. It was generated by starting with a conditionally unstable atmosphere, to which heat is supplied at the bottom in a random manner. Grid points are spaced at 200 m intervals, both in vertical and horizontal direction. The integration was performed with a time step of 10 seconds. Deep convective clouds of the type shown appeared after a few hours of simulated time.

The most striking feature in Figure 10 is the presence of very large horizontal gradients in vertical velocity. The cloud is 'fed' by an updraught of about 8 m/s, and produces sharp downdraughts at its edges. The reason for this is the evaporation of large amounts of liquid water, which cools the air very rapidly (note the dips in the isotherms near the cloud edge). Such downdraughts are a real feature: they are well known by glider pilots ! In some cases, mostly in connection with thunderstorms, downdraughts are so strong that they seriously damage obstacles at the surface.

The cloud structure shown in Figure 10 agrees well with observations made from aircraft and balloons. However, when cumulus clouds reach a stage in which large amounts of precipitation are produced, they attain an essentially three-dimensional structure (in which vortex stretching, which cannot be simulated in two dimensions, plays an important role). Numerical simulation of heavy showers is therefore only possible with three-dimensional models. It then also becomes necessary to take into account the effect of horizontal pressure variations and compressibility effects.

Such models exist and are currently being used for case studies of severe thunderstorms and squall lines (e.g. Miller, 1978).

8. ORGANIZATION OF CONVECTIVE CLOUDS

From many observations it is known that convective clouds tend to form groups. In many cases this will be related to varying properties of the underlying surface (e.g. bare sand is superior in producing thermals that may initiate clouds), but even for uniform surface conditions grouping of cumulus clouds occurs. Such uniform conditions are for example found over sea water.

The cell and roll patterns appearing in Figure 9 suggest similarity to classical Rayleigh-Bénard convection. Krishnamurti (1975) has investigated this point in some detail. Her results were not very convincing, however. The horizontal dimension of rolls and cells found in the atmosphere (as compared to the depth) is so large that it can hardly be explained by the classical theory of convection. In addition, the cloudy regions (shown in black in Figure 9) are not associated with one single updraught, but consist of many individual clouds having their own up- and downdraughts. This is known from aircraft measurements and can in fact be seen from the ground. So it is better to state that clouds group together in such a way that cell and roll patterns appear rather than to interpret each cell or roll as one smooth circulation.

Again, numerical simulation may help a lot in understanding the grouping of convective clouds. The problem here is that a large model domain is needed to study the formation of groups. In three dimensions this leads to memory and central-processor time requirements that are simply too large. In two dimensions (vertical plane), explicit calculations of cloud organization now become possible. Figure 11 provides an example. It shows in a running-time diagram how a random cloud pattern transforms to an organized pattern (black in the figure means that liquid water is present at some height). In this numerical experiment (described in Van Delden and Oerlemans, 1982) the grid had 20 points in the vertical and 300 points in the horizontal direction, corresponding to distances of 4 and 60 km. Heating at the bottom grid points was purely random, so organization must come from internal processes. Apparently, such processes were present.

A closer look at model results of this type strongly suggest that downdraughts created at cloud edges form a strong dynamical forcing (when hitting the ground, they enforce updraughts). So a deep cloud tends to generate new clouds in its environment. The cloud-scale (≈5 km) motions mechanically force a larger scale (30 km) circulation, which tends to maintain regions of high relative humidity, in which a cloud population can easily maintain itself. In this way the system creates two dominant horizontal length scales: the cloud scale determined by the depth of the unstable layer and the eddy diffusivity,

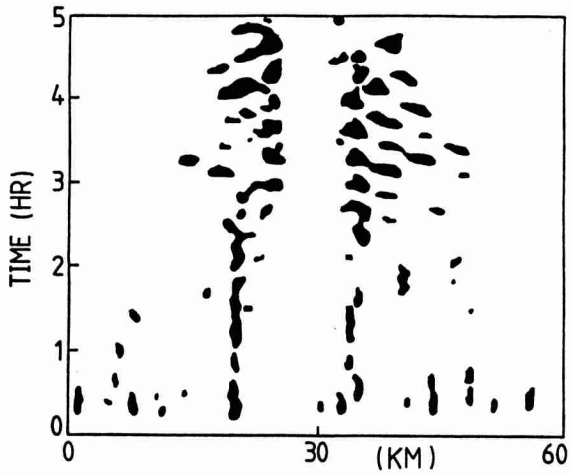

Figure 11. Running-time diagram of cloud formation in a two-dimensional numerical model.

and the cell scale determined by the interaction of flow pattern and moisture field.

There is another way to look at the phenomenon of cloud organization. The probability that deep convective clouds form increases very rapidly with relative humidity. Deep clouds are very effective in creating cloud-scale kinetic energy and in transporting heat upwards, far more effective than shallow clouds. So a maximizing principle suggests itself: more kinetic energy (the best quantity to measure the convective activity) is generated if the moisture, and therewith the conditional instability, can be concentrated in specific regions, so that deep clouds can develop. It seems that nature follows this principle. However, a specific minimum level of convective activity is required to initiate the cell-scale circulation. In case of weak forcing, or in a comparatively stable atmosphere, cell or roll patterns cannot be established.

Grouping of clouds has many interesting aspects, and numerical experimentation on this topic has only just begun. Cloud pictures from geostationary satellites (e.g. METEOSAT), which have a high resolution in time, now become available in large amounts. Systematic investigation of these pictures, together with carefully designed model experiments, will undoubtly lead to a better understanding of the dynamics of cloud groups.

ACKNOWLEDGEMENTS

Thanks go to Prof. Cor Schuurmans for useful criticism on the manuscript, and to the editor of 'Contributions to Atmospheric Physics' for his permission to reproduce Figures 10 and 11.

REFERENCES

Charney, J.G., The dynamics of long waves in a baroclinic westerly current, J. Meteor., vol. 4, pp. 135-162, 1947.

Driedonks, A.G.M., Dynamics of the well-mixed atmospheric boundary layer, Scientific Report No. 81-2, Royal Netherlands Meteorological Institute, De Bilt, 1981.

Eady, E.T., Long waves and cyclone waves, Tellus, vol. 1, pp. 35-52, 1949.

Gilmore, R., Catastrophe theory for scientists and engineers, pp. 1-666, John Wiley, New York, 1981.

Holton, J.R., An introduction to dynamic meteorology, pp. 1-319, Academic Press, New York, 1972.

Krishnamurti, R., On cellular cloud patterns. Part 3: applicability of the mathematical and laboratory models, J. Atmos. Sci., vol. 32, pp. 1373-1383, 1975.

Lorenz, E.N., The nature and cause of the general circulation of the atmosphere, pp. 1-161, World Meteorological Organization, Geneva, 1967.

Manabe, S. and Wetherald, R., Thermal equilibrium of the atmosphere with a given distribution of relative humidity, J. Atmos. Sci., vol. 24, pp. 241-259, 1967.

Miller, M.J., The Hampstead storm: a numerical simulation of a quasi-stationary cumulonimbus system, Quart. J. Roy. Met. Soc., vol. 104, pp. 413-427, 1978.

Oerlemans, J., and Van den Dool, H.M., Energy-balance climate models: stability experiments with a refined albedo and updated coefficients for infrared emission, J. Atmos. Sci., vol. 35, pp. 371-381, 1978.

Oort, A.H., On estimates of the atmospheric energy cycle, Mon. Weather Rev., vol. 92, pp. 483-493, 1964.

Paltridge, G.W., and Platt, C.M.R., Radiative processes in meteorology and climatology, pp. 1-318, Elsevier, Amsterdam, 1976.

Ramanathan, V., The role of ocean-atmosphere interactions in the CO_2 climate problem, J. Atmos. Sci., vol. 38, pp. 918-930, 1981.

Stone, P.H., Baroclinic adjustment, J. Atmos. Sci., vol. 35, pp. 561-571, 1978.

Tennekes, H., A model for the dynamics of the inversion above a convective boundary layer, J. Atmos. Sci., vol. 30, pp. 558-567, 1973.

Thom, R., Stabilité structurelle et morphogénèse, Benjamin, New York, 1972.

Van Delden, A., and Oerlemans, J., Grouping of clouds in a numerical cumulus convection model, Contr. Atmos. Phys., in the press.